Comparison of Inverse Structural Filter (ISF) and Sum of Weighted Accelerations Technique (SWAT) Time Domain Force Identification Methods

Matthew S. Allen* and Thomas G. Carne.†
Sandia National Laboratories, Albuquerque, New Mexico, 87185, USA

Two time domain force identification methods are compared to the standard frequency domain technique in terms of accuracy and sensitivity to errors and a number of extensions are presented which improve their accuracy. Much of the previous in research force reconstruction has focused on frequency domain methods, yet there are applications in which a real time estimate of the input forces is desired or when time data is available over such a short duration that frequency domain methods cannot be applied effectively. Furthermore, the challenges inherent to the inverse problem are manifested differently in the time domain, so it is possible that accuracy and robustness could improve by considering both time and frequency domains. This work reviews two time domain force identification methods, the Inverse Structural Filter (ISF), which is based on a discrete time, state space representation of the dynamics, and the Sum of Weighted Accelerations Technique (SWAT), which is based upon modal filtering. Both of these techniques make use of a modal description of the structural dynamics, so particular attention is given to identifying an adequate model. Actual test data from a free-free beam is used to compare the methods. The application reveals some of the deficiencies of the methods and a number of extensions of the ISF method are presented which greatly improve its performance at certain frequencies and are perhaps easier to apply than the original ISF method. The results of a Monte Carlo simulation are also presented, illustrating the sensitivity of the methods to errors in the modal parameters of the forward system. The results suggest that an accurate description of the forces can be found using the structural response in many important cases, especially when the forces have short duration or relatively smooth spectra in the frequency band of interest.

I. Introduction

There are countless applications in which it is difficult or impossible to directly measure the dynamic forces acting on a structure, yet knowledge of these forces is vital for analysis and design optimization. In some of these cases it is possible to measure the response of the structure to the unknown forces. Numerous previous works have studied the feasibility of using a structure's response to identify the forces acting on it, in effect, using the structure as its own force transducer [1]. This inverse problem is usually described as ill posed [1, 2]. Its solution can also be very sensitive to small inaccuracies in the data [3-5]; seemingly insignificant errors in the forward structural dynamic model can result in large errors in the computed forces. However, one should be careful and not admit defeat to easily; the forward and inverse problems are different and one should expect that different structural dynamic characteristics will be important in each.

The classical approach to force reconstruction is to use a frequency domain technique in which the discrete Fourier transform of the measured responses is multiplied by the inverse (or pseudo-inverse) of the FRF matrix, yielding an estimate of the forces acting on the system. Frequency domain force reconstruction has been studied by a number of researchers [1, 3, 4, 6, 7] The recent work by Hundhausen *et al* [2] provides a comprehensive review.

It is preferable in some applications to have a time domain algorithm capable of estimating the forces acting on a structure in real time. For example, these forces may be required for system control purposes, or the available data may be of such short duration that leakage renders frequency domain processing inaccurate. Also, the challenges in

* Postdoctoral Appointee, Dept. 1526, P.0. Box 5800, MS 0557, Member AIAA.
† Distinguished Member of Technical Staff, Dept. 1525, P.0. Box 5800, MS 0557, Member AIAA.

the inverse problem are manifested differently in the time domain, so it is possible that more accurate or robust solutions could be found there. However, it appears that time domain force identification has not been studied as widely as has the frequency domain dual.

This work evaluates the relative merits of two time domain force reconstruction techniques, the Sum of Weighted Accelerations Techinque (SWAT) and the Inverse Structural Filter (ISF) algorithm. The algorithms are tested on data measured from a simple aluminum beam with free-free boundary conditions. The results obtained by the time domain algorithms are also compared to those obtained by the classical frequency domain technique, and the relative merits of each method are enumerated.

Some deficiencies in these methods were noted in these comparisons and a number of modifications to the algorithms were explored in an effort to improve their performance. Many variations on the ISF algorithm were explored, some of which were found to significantly reduce errors in the estimated force spectrum at certain frequencies. These alternative methods also simplify the process of generating an ISF system since they rely on the forward dynamic model for the system and many well known methods are available for finding such a model. Thus one can avoid the more involved process of directly identifying the ISF from measurements that was used by Kammer [5, 8-10]. The more fruitful of the extensions to the ISF method are discussed and some directions for future research are highlighted. The SWAT algorithm was also explored somewhat. The performance of the algorithm is demonstrated as the number of modes in the frequency band of interest varied for a fixed number of sensors. The inclusion of the residual flexibility or out of band modes was also explored and found to improve the results somewhat.

The primary contributions of this work are the following. First, a detailed evaluation of two major time domain force reconstruction techniques using laboratory data. Second, this work provides a comparison between the time domain and frequency domain techniques. This is especially valuable for the ISF algorithm, which has not previously been tested against classical techniques. Third, the robustness of all of the methods to errors in the modal parameters of the forward system is studied through a Monte-Carlo simulation. Finally, new variations on the ISF algorithm are proposed and investigated, which significantly improve its performance.

The next section presents a review of time domain force identification methods and discusses some details of the implementation of SWAT and ISF. In Section III, these algorithms are applied to data from an aluminum beam, which is suspended to simulate free boundary conditions. Some conclusions are presented in Section IV.

II. Time Domain Force Identification

A few researchers have proposed time domain techniques for identifying the forces acting on a structure. Some of these are referenced in [2]. For example, Hollandsworth and Busby [11] presented an algorithm in 1989. Law and Chan [12] presented an algorithm for identifying moving loads, i.e. the problem of a car on a bridge. The work here focuses on two time domain techniques: the Sum of Weighted Accelerations Technique, and the Inverse Structural Filter. Most of the other time domain force identification techniques in the literature are, in essence at least, very similar to one of these two [11-13]. These two methods were preferred because they are well developed and because elegant theory exists for predicting their performance.

A. Sum of Weighted Accelerations (SWAT)

The Sum of Weighted Accelerations Technique (SWAT) was presented by Carne *et al* [14], although the method had been developed previously by Gregory, Priddy and Smallwood [15, 16]. It has been successfully applied to a number of systems [17-19]. The technique is based upon the concept of a modal filter. The rigid body mode shapes, along with the mode shapes of the elastic modes in the frequency band of interest are used to construct a spatial filter that removes the flexible modes from the response, leaving only the rigid body accelerations. This spatial filter is simply a weighting vector that isolates the rigid body accelerations in the response. If the mass properties of the structure are known, the rigid body accelerations can be multiplied by the mass properties to obtain an estimate of the forces and moments acting at the body's center of gravity.

In some cases the free, unforced response, which is a linear combination of the elastic mode shapes, can be used to generate an adequate spatial filter (i.e. the SWAT-TEEM algorithm [14, 19]). One limitation of the SWAT algorithm is that it determines the equivalent forces and moments that, if applied at the center of mass, would cause the same acceleration of the center of mass, and does not identify the spatial distribution of the applied forces. If the location at which the force is applied is known and the number of applied forces is less than or equal to the number of rigid body modes, this may be sufficient to determine the individual forces. Genaro and Rade [13] presented an extension of SWAT that can identify the forces at individual response points provided that the number of modes in the frequency band of interest exceeds the number of forces desired. Another limitation of the SWAT algorithm is

that it requires that the number of sensors be at least as great as the number of rigid body modes plus the number of elastic modes and that the sensors are well placed so that the filtering problem is well conditioned.

The SWAT algorithm is derived in [14, 17, 18] and explained in the context of the modal filter. An alternate derivation will be summarized here. We begin by approximating the measured acceleration as a sum of modal contributions as follows

$$\{a\} = [\Phi]\{\ddot{\eta}\} \tag{1}$$

where $\{a\}$ is an N_0x1 vector of accelerations at the measurement points, $\{\eta\}$ is an Nx1 vector of modal displacements, $[\Phi]$ is an N_0xN matrix of mode shapes and N_o and N are the number of measurement points and modes respectively. An N_oxN_{RB} weighting matrix [W] is sought that, when multiplied with the measured accelerations, extracts an N_{RB}x1 vector of rigid body accelerations $\{a_{RB}\}$.

$$\{a_{RB}\} = [W]^T \{a\} \tag{2}$$

If the rigid body mode vectors are mass normalized and assigned to the leading columns of $[\Phi]$, then equation (1) can be rewritten as

$$\{a\} = \begin{bmatrix} [\Phi_{RB}] & [\Phi_e] \end{bmatrix} \begin{Bmatrix} \{a_{RB}\} \\ \{\ddot{\eta}_e\} \end{Bmatrix} \tag{3}$$

where the matrices represent the rigid body and elastic modes respectively and $\{\eta_e\}$ is the vector of elastic modal coordinates corresponding to the modes in $[\Phi_e]$. Combining equations (3) and (2) and with the requirement that $[W]^T$ nullify the elastic modes while extracting the rigid body accelerations yields

$$\begin{aligned} [W]^T \begin{bmatrix} [\Phi_{RB}] & [\Phi_e] \end{bmatrix} &= \begin{bmatrix} [I]_{N_{RB} \times N_{RB}} & [0]_{N_e \times N_{RB}} \end{bmatrix} \\ [W] &= \left(\begin{bmatrix} [\Phi_{RB}] & [\Phi_e] \end{bmatrix}^T \right)^+ \begin{bmatrix} [I]_{N_{RB} \times N_{RB}} \\ [0]_{N_e \times N_{RB}} \end{bmatrix} \end{aligned} \tag{4}$$

where $()^+$ denotes the pseudo-inverse. One would expect to be able to find a solution that nullifies the elastic modes (or extracts the pure rigid body accelerations) whenever the N_{RB} vectors comprising [W] can be extracted from the null space of the transpose of the elastic mode matrix $[\Phi_e]^T$. This will always be possible whenever $N_o \geq N+N_{RB}$. One should recall that equation (1) is an approximation because any continuous system has, in reality, an infinite number of modes.

The rigid body accelerations are multiplied by the rigid body mass properties yielding the sum of the forces applied to the body. One should consult the derivations in [14, 17, 18] for further insight. The derivation there sheds some light on the importance of sensor selection by casting the algorithm as a variant of the modal filter.

B. Inverse Structural Filter (ISF)

Recently, a time domain algorithm dubbed the Inverse Structural Filter (ISF) was presented by Steltzner and Kammer [5, 8-10]. In some incarnations it can be considered a time domain dual to the classical frequency domain algorithms. The discrete time equations of motion are inverted resulting in a dynamic system that takes the structure's response as input and returns an estimate of the forces acting on the structure as output. Kammer and Steltzner have investigated various techniques for overcoming the ill-conditioning [5] and instability [10] that can result.

The basic ISF algorithm can be derived easily beginning with the familiar linear, state-space, discrete time representation for a dynamic system.

$$\begin{aligned}\{x_{k+1}\} &= [A]\{x_k\} + [B]\{u_k\} \\ \{y_k\} &= [C]\{x_k\} + [D]\{u_k\}\end{aligned} \tag{5}$$

where the state vector $\{x\}$ is $Nx1$, the input vector $\{u\}$ is $N_i x1$, and the output vector $\{y\}$ is $N_o x1$. The index k refers to the kth time step for which $t_k = kT_s$ where T_s is the sample increment or time between successive time samples. For structural dynamic systems, the forces acting on a structure at a set of points are typically the inputs, and the displacement, velocity, or acceleration measured at a set of points are considered the outputs. Peeters [20] gives a good review of various forms of the state-space equations for continuous and discrete time dynamic systems, as well as their relationships to the familiar modal and structural-dynamic (i.e. M,C,K) representations. It is important to note that the discrete time system reproduces the response of its continuous time dual exactly (at the sample instants) only if the response obeys the assumption used in deriving the discrete time model. For example, the zero order hold (ZOH) assumption is typically used, which assumes that the input is constant between sample instants. This is an important detail to consider, especially since most of the data acquisition hardware used in structural dynamics uses a different (band-limited) assumption. Fortunately the distinction is not too important so long as the sample rate is considerably higher than the maximum frequency of interest.

Steltzner and Kammer noted that it is possible to use a pseudo-inverse to invert the state space representation in eq. (5) as follows

$$\begin{aligned}\{x_{k+1}\} &= [\hat{A}]\{x_k\} + [\hat{B}]\{y_k\} \\ \{u_k\} &= [\hat{C}]\{x_k\} + [\hat{D}]\{y_k\} \\ \hat{A} &= A - BD^{+}C \quad \hat{B} = BD^{+} \\ \hat{C} &= -D^{+}C \quad \hat{D} = D^{+}\end{aligned} \tag{6}$$

where $()^{+}$ denotes the pseudo-inverse. Equation (6) represents a discrete time dynamic system that takes the response $\{y\}$ as input and returns an estimate of the forces $\{u\}$ acting on the system as output. This can also be expressed as a discrete filter that acts on the sampled response measurements returning a sampled (i.e. ZOH) estimate of the forces.

While Steltzner and Kammer derived the ISF as described above, they did not actually use this procedure to implement the ISF. Instead, they presented an algorithm that computes the Markov parameters of the ISF directly from response data [10]. The next section explores the alternative of generating an inverse structural filter from modal parameters obtained in a standard modal test using a modal representation of equation (6).

1. Deriving an ISF from Modal Parameters

The matrices comprising an ISF system can be computed in a number of ways, a few of which will be explored in this paper. We assume that the Frequency Response Function (FRF) has been measured and fit to a state-space modal model according to the following standard definition

$$[H(\omega)]_{N_o \times N_i} = \sum_{r=1}^{N/2} \left(\frac{[A]_r}{i\omega - \lambda_r} + \frac{[A^*]_r}{i\omega - \lambda^*_r} \right) \tag{7}$$

where $()^{*}$ denotes the complex conjugate, $H(\omega)$ is the FRF matrix at frequency ω, λ_r is the modal eigenvalue $\lambda_r = -\zeta_r\omega_r + \omega_r(1-\zeta_r^2)^{1/2}$, where ζ_r is the modal damping ratio and ω_n the modal natural frequency for the rth mode of vibration. If the mode vectors are normalized as described by Ginsberg [21], then the residue matrices $[A]_r$ can be defined in terms of the displacement portion of the state space mode vector $\{\psi\}_r$ as follows

$$[A]_r = \lambda_r \{\psi_{resp}\}_r \{\psi_{drive}\}_r^{T} \tag{8}$$

where the subscripts denote the mode vector partitioned into the drive and response locations. If the forces are applied at a subset of the response locations, then these can be expressed as

$$\{\psi\}_r = \{\psi_{resp}\}_r$$
$$\{\psi_{drive}\}_r^T = \{\psi\}_r^T [F_{in}] \tag{9}$$

where $[F_{in}]$ is typically a $N_o x N_i$ matrix of ones and zeros that selects the subset of the response locations at which forces are applied. One can use the Laplace domain representation of eq. (7) to show that the following state space system generates the Frequency response function in eq. (7).

$$\begin{aligned}
&\{\dot{x}\} = [A_c]\{x\} + [B_c]\{u\} \\
&\{y\} = [C_c]\{x\} \\
&[A_c] = \begin{bmatrix} \Lambda & \\ & \Lambda^* \end{bmatrix} \quad [B_c] = \begin{bmatrix} \Psi\Lambda & \Psi^*\Lambda^* \end{bmatrix}^T [F_{in}] \\
&[C_c] = \begin{bmatrix} \Psi & \Psi^* \end{bmatrix}
\end{aligned} \tag{10}$$

In the preceding equation, $[\Lambda]$ is a diagonal matrix containing the eigenvalues in ascending order and the columns of $[\Psi]$ contain the mode vectors $\{\psi\}_r$ in the same order as the eigenvalues. The subscript 'c' denotes that these are the state space matrices for the continuous time representation, in contrast to the discrete time matrices in eq. (5).

In many applications one actually measures acceleration. One can modify the representation in eq. (10) to arrive at a state space representation for acceleration measurements by taking two derivatives of the output equation and substituting the derivative of the state equation. The following state space representation results.

$$\begin{aligned}
&\{\ddot{x}\} = [A_c]\{\dot{x}\} + [B_c]\{\dot{u}\} \\
&\{\ddot{y}\} = [C_c]\{\ddot{x}\} = [C_c]\left([A_c]\{\dot{x}_c\} + [B_c]\{\dot{u}\}\right) \\
&\{\ddot{y}\} = [C_A]\{\dot{x}\} + [D_A]\{\dot{u}\} \\
&[C_A] = \begin{bmatrix} \Psi\Lambda & \Psi^*\Lambda^* \end{bmatrix} \quad [D_A] = [C_c][B_c] \\
&[D_A] = 2\,\mathrm{Re}\left(\Psi\Lambda\Psi^T\right)[F_{in}]
\end{aligned} \tag{11}$$

The new state vector is the derivative of the state vector in eq. (10). The input vector in eq. (11) is the derivative of the applied forces. Once inverted, the system in eq. (11) will estimate the derivative of the input forces from the acceleration measurements. These estimates must then be integrated numerically to obtain at the input forces.

A discrete time dual to the system representation in eq. (11) must be obtained in order to generate a discrete time inverse structural filter using eq. (6). The following discrete time representation will exactly reproduce the output of the continuous time system at the sample instants, if the input is constant between samples (zero-order-hold (ZOH) approximation).

$$\begin{aligned}
&\{x_{k+1}\} = [A]\{\dot{x}_k\} + [B]\{\dot{u}_k\} \\
&\{\ddot{y}_k\} = [C]\{\dot{x}_k\} + [D]\{\dot{u}_k\} \\
&[A] = \exp(A_c T_s) \quad [B] = [A_c]^{-1}\left[\exp(A_c T_s) - [I]\right][B_c] \\
&[C] = [C_A] \quad [D] = [D_A]
\end{aligned} \tag{12}$$

Note that because $[A_c]$ is diagonal, the matrix exponential of $[A_c]$ is a diagonal matrix with the discrete time eigenvalues $z_r=exp(\lambda_r T_s)$ along its diagonal. The same discrete time system matrices *[A], [B], [C]* and *[D]* can be obtained from the continuous time ones using the 'c2d' function in Matlab's control system toolbox.

2. Improving Performance: Direct Transmission Matrix [D]

One of the primary challenges with the Inverse Structural Filter method is obtaining a stable ISF. If any of the eigenvalues of the ISF system in eq. (6) are unstable, the estimated forces might tend towards infinity when the ISF is applied to the measured responses. This section presents a few tricks that can help in finding a stable ISF.

For example, the authors have found that the representation in eq. (12) resulted in an unstable inverse structural filter when applied to the beam data discussed in the following section, while a slightly modified discrete time representation gave better performance. The modified representation is obtained by stepping the output forward one sample and neglecting the direct transmission matrix *[D]*, resulting in the following delayed state space representation.

$$\begin{aligned}
\{x_{k+1}\} &= [A]\{\dot{x}_k\} + [B]\{\dot{u}_k\} \\
\{\ddot{y}_{k+1}\} &= [C]\{\dot{x}_{k+1}\} + \cancelto{0}{[D]}\{\dot{u}_{k+1}\} \\
\{\ddot{y}_{k+1}\} &= [C]\left([A]\{\dot{x}_k\} + [B]\{\dot{u}_k\}\right) \\
\{\ddot{y}_{k+1}\} &= [C_d]\{\dot{x}_k\} + [D_d]\{\dot{u}_k\} \\
[C_d] &= [C][A] \quad [D_d] = [C][B]
\end{aligned} \tag{13}$$

The ISF for this system, generated using eq. (6), estimates the input at time t_k from the response at the next time instant t_{k+1}. One can heuristically justify omitting the direct transmission matrix [D] on the grounds that for a lightly damped system the real parts of *[Λ]* and *[Ψ]* tend to be small, so the real part of the triple $[\Psi][\Lambda][\Psi]^T$ is also likely to be small for lightly damped structures and based on less accurately estimated quantities, such as the modal damping ratios and the real parts of the state space mode vectors.

3. Improving Performance: Delayed Multistep ISF (DMISF)

In [10], Steltzner and Kammer found that it was possible to create a non-causal ISF that was more stable and/or more accurate than the standard one. (The non-causal ISF used future values of the response to estimate the forces at a given time.) In that same spirit, if one can tolerate a delay before the forces are estimated, then it is sometimes possible to improve the performance of the ISF using the following method.

Consider forward state equation (13). The following modified output equation results after stacking the input and output for various time instants.

$$\begin{aligned}
\begin{Bmatrix} \{\ddot{y}_{k+1}\} \\ \{\ddot{y}_{k+2}\} \\ \vdots \\ \{\ddot{y}_{k+p}\} \end{Bmatrix} &= \begin{bmatrix} [C_d] \\ [C_d][A] \\ \vdots \\ [C_d][A]^{p-1} \end{bmatrix} \{\dot{x}_k\} + \begin{bmatrix} [D_d] & [0] & \cdots & [0] \\ [C_d][B] & [D_d] & \ddots & [0] \\ \vdots & \ddots & \ddots & [0] \\ [C_d][A]^{p-2}[B] & [C_d][A]^{p-3}[B] & \cdots & [D_d] \end{bmatrix} \begin{Bmatrix} \{\dot{u}_k\} \\ \{\dot{u}_{k+1}\} \\ \vdots \\ \{\dot{u}_{k+p-1}\} \end{Bmatrix}, \\
\{\ddot{y}^S_{k+1}\} &= [C_{dm}]\{\dot{x}_k\} + [D_{dm}]\{\dot{u}^S_k\}
\end{aligned} \tag{14}$$

The state equation must be modified slightly to accommodate the new definition of the output and input

$$\begin{aligned}
\{x_{k+1}\} &= [A]\{\dot{x}_k\} + [B][P]\{\dot{u}^S_k\} \\
[P] &= \begin{bmatrix} [I] & [0] & \cdots & [0] \end{bmatrix}
\end{aligned} \tag{15}$$

An ISF can be generated from this system representation that estimates the input at time instants t_k to t_{k+p-1} from the output at time instants t_{k+1} to t_{k+p}. This can be applied to the output at t_k to t_{Nt-p} resulting in multiple estimates for each of the input forces. The most important feature of this method is that it sometimes produces a stable ISF system when that produced by eq. (13) is unstable. Furthermore, the examples in the following section will show that this method can be slightly more accurate. This algorithm will be referred to as the delayed, multi-step ISF or DMISF.

C. Frequency Domain Inverse Method

By far the most common inverse method used is the frequency domain inverse method. This is based on the following relationship between force and response.

$$\underset{N_o\times 1}{\{X(\omega)\}} = \underset{N_o\times N_i}{[H(\omega)]}\underset{N_i\times 1}{\{F(\omega)\}} \tag{16}$$

The use of frequency domain data implicitly assumes that the responses have been measured over a sufficiently long time window and transferred to the frequency domain via a Discrete Fourier Transform.

Typically, the number of output or response locations exceeds the number of force or input locations, so the inverse problem is overdetermined. The forces are obtained by multiplying both sides of the equation by the pseudo-inverse of $[H(\omega)]$.

$$\underset{N_i\times 1}{\{F(\omega)\}} = \underset{N_i\times N_o}{[H(\omega)]^{+}}\underset{N_o\times 1}{\{X(\omega)\}} \tag{17}$$

The primary difficulty in applying this method stems from the fact that the FRF matrix tends to be dominated by a rank-one component corresponding to a single mode near the natural frequencies of a system. As a result, the inverse of the FRF matrix can be ill conditioned near the natural frequencies of the system thus amplifying the effect of measurement errors [4].

The FRF matrix in eq. (16) could consist of measured data, or could be reconstructed from a modal model for the system. The latter approach was used in the results that follow to facilitate comparison with the SWAT and ISF methods. As a result, both the frequency domain inverse method and the time domain methods are constructed from identical data, the modal model for the system.

III. Experimental Results

The data presented in this section was taken from a 183 cm long aluminum beam, suspended by bungee cords to simulate free-free boundary conditions. The beam cross section was 2.5 cm high by 3.8 cm wide. Seven pairs of accelerometers were mounted along the length of the beam, spaced 30.5 cm apart. Each pair contained one accelerometer mounted in the vertical direction and one in the axial direction.

An instrumented hammer was used to excite the beam and record the force imparted. The measured force and response spectra were used to estimate the frequency response function of the beam, which was processed using two modal parameter identification algorithms: the Synthesize Modes and Correlate Algorithm (SMAC) [22, 23], and the Algorithm of Mode Isolation (AMI) [24-26]. These returned a set of modal parameters describing the dynamics of the beam from 0 Hz to 1500 Hz. Beyond 1500 Hz the excitation was relatively weak and the FRFs were difficult to curve fit. The modal parameters identified by both of these algorithms were similar. The results of the AMI algorithm were used as described subsequently as input data for the various force identification algorithms. The force identification algorithms differ in the amount of information needed as well as their sensitivity to inaccuracies in the data. For this reason, some additional details regarding the curve fitting procedure will be furnished in the following subsections.

A separate set of data was also taken in which the beam was excited once with an instrumented hammer and the response recorded. A number of force reconstruction algorithms were then applied to the response data, as described subsequently, where in each case the reconstructed force is compared to the force measured by the hammer.

A. Sum of Weighted Accelerations Technique (SWAT)

The Algorithm of Mode Isolation (AMI) was used to find the modal parameters for the beam. Figure 1 compares the measured frequency response function at the drive point with AMI's reconstruction. The algorithm described in [27] was modified to force a model with real modes on the data. The measured and reconstructed FRFs agree quite well, although the zeros of the FRF at low frequencies have not been identified very accurately. Figure 2 shows composite FRFs of the data, AMI's reconstruction, and the difference between the two. (A composite FRF is defined as the average of the magnitude of all of the FRFs.) Once again the agreement is quite good, although the difference plot does reveal errors at each of the natural frequencies of about one order of magnitude less than the measured FRF magnitude. When complex modes were fit to the data these errors were virtually eliminated, as will be illustrated in the following section.

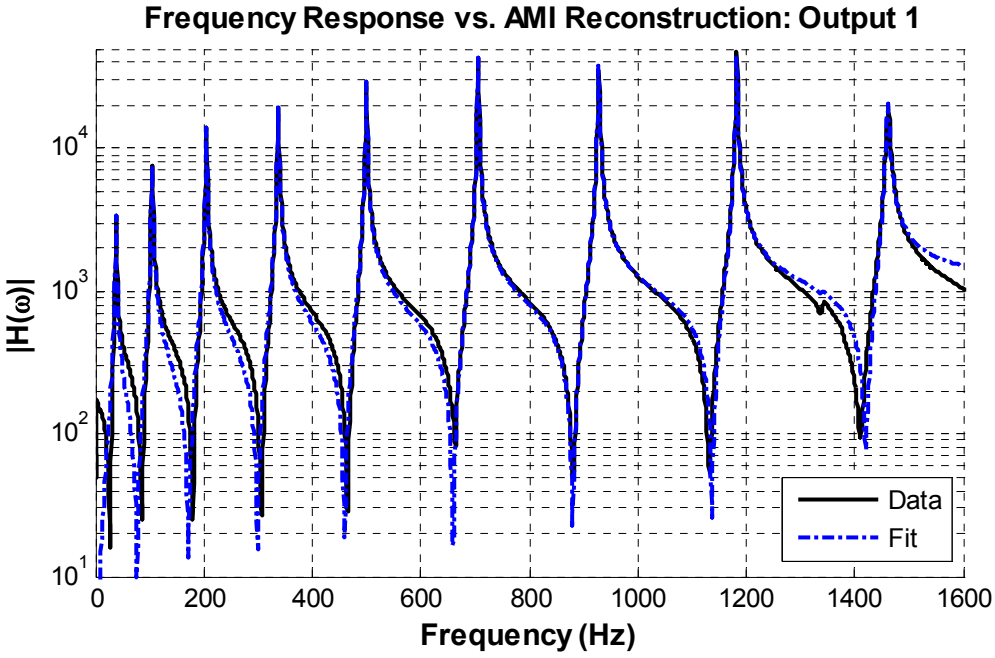

Figure 1: Measured Drive Point FRF $H_{1,1}(\omega)$ vs. AMI Reconstruction – Real Modes.

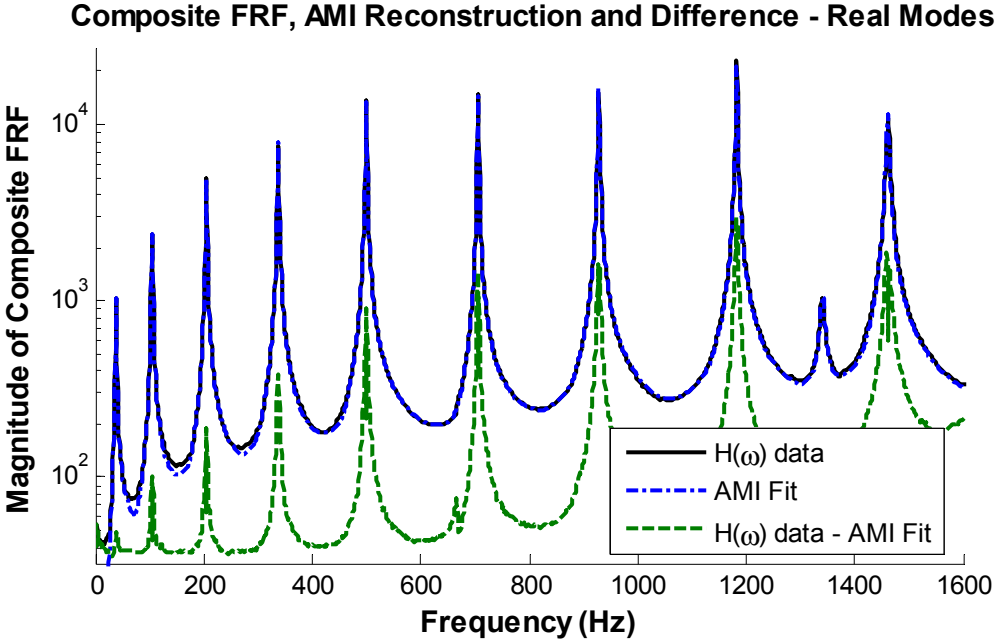

Figure 2: Composites of Measured FRFs, AMI's Reconstruction and of the difference between the two – Real Modes.

Figure 3 shows a plot of the Modal Assurance Criterion Matrix or MAC Matrix [28] of the modes identified by AMI. (The MAC between two vectors gives an indication of their linear independence. A value of 0 indicates perfect independence, or vectors that are orthogonal in a Euclidean sense, while a value of 1 indicates that the vectors are multiples of one another.) The off-diagonal MAC values (i.e. the MACs between the different mode vectors) are above 0.5 for a number of the mode vector pairs, suggesting that a larger number of measurement points may be needed to accurately distinguish the mode shapes from one another.

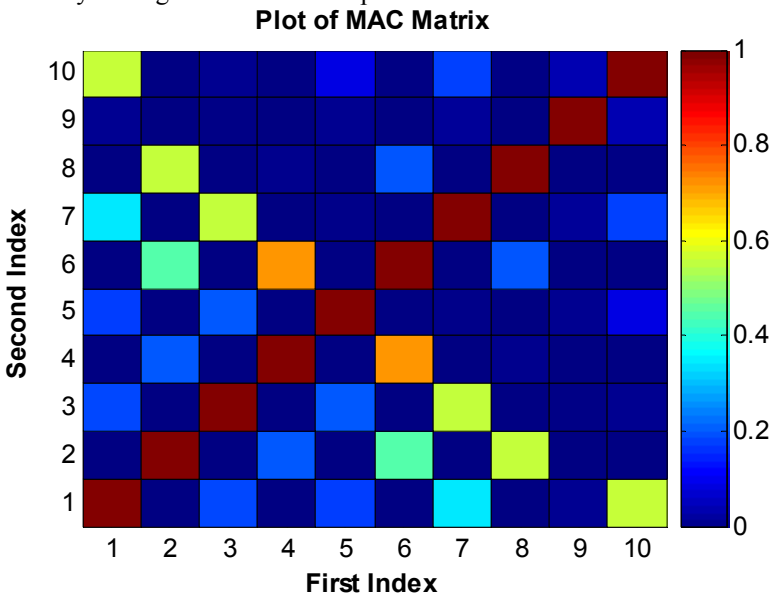

Figure 3: Plot of MAC matrix between modes identified by AMI – Real Modes.

The SWAT algorithm can be applied to the measured FRFs resulting in what has been called an FRF of the SWAT degrees of freedom or SWAT FRFs [14, 17]. The SWAT FRFs are computed by multiplying the SWAT weights with the measured FRF matrix. Since the measured FRFs represent the response due to a flat, unit force (or unit impulse force), the resulting SWAT FRFs should be constant for all frequencies. Visual inspection of the SWAT FRF gives a good indication of the ability of SWAT to isolate the rigid body accelerations of the structure. Figure 4 shows the SWAT FRFs for the two dominant rigid body modes present in the data, rigid body translation in the vertical direction and rigid body rotation. The SWAT FRFs are essentially flat up to about 600 Hz. They clearly indicate that one should not apply SWAT (using this sensor set) without first low pass filtering the response data to minimize the frequency content to below about 1000 Hz. Another alternative would be to add more sensors to eliminate the modes in the frequency band of interest.

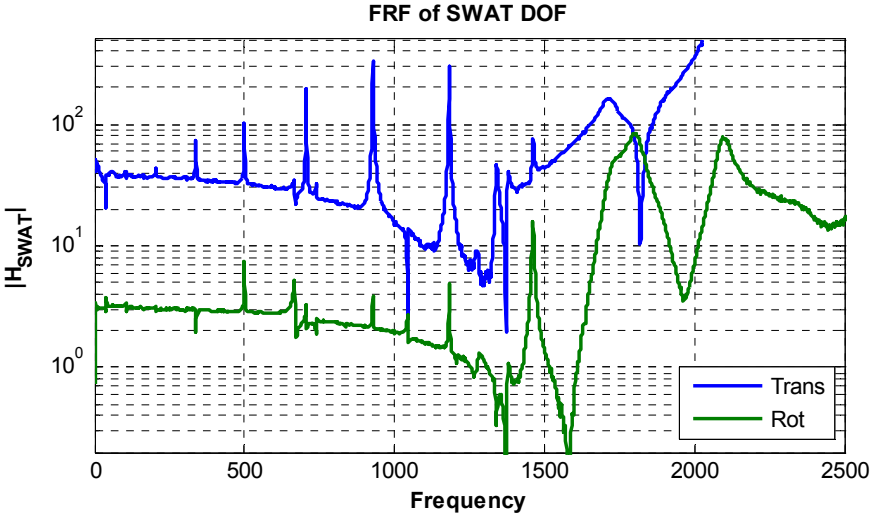

Figure 4: FRF for SWAT degrees of freedom, rigid body translation and rigid body rotation (or pitch.)

Figures 5 and 6 show the force identified by SWAT from the response data for a vertical input force (perpendicular to the axis of the beam) at the first degree of freedom. The response data has been low-pass filtered with a cutoff frequency of 1500 Hz. Recall that the SWAT FRFs indicated that the forces identified by SWAT were not likely to be very accurate above 1000Hz. Higher frequencies were included in the following so that these results could be compared with those derived using the ISF and frequency domain inverse methods later. In practice one should always limit the bandwidth of the responses to the flat region of the SWAT FRFs prior to applying SWAT or augment the sensor set as discussed previously.

SWAT identified the sum of the external forces acting on the center of mass of the beam, which includes the vertical force at and the moment about the center of mass in this case. The location of the applied force is known, so each of these forces can be considered an estimate of the applied force. These two estimates were averaged to yield a single estimate for the force acting at the 1st measurement point. Figures 5 and 6 compare this estimated force with the measured force in the time and frequency domains respectively.

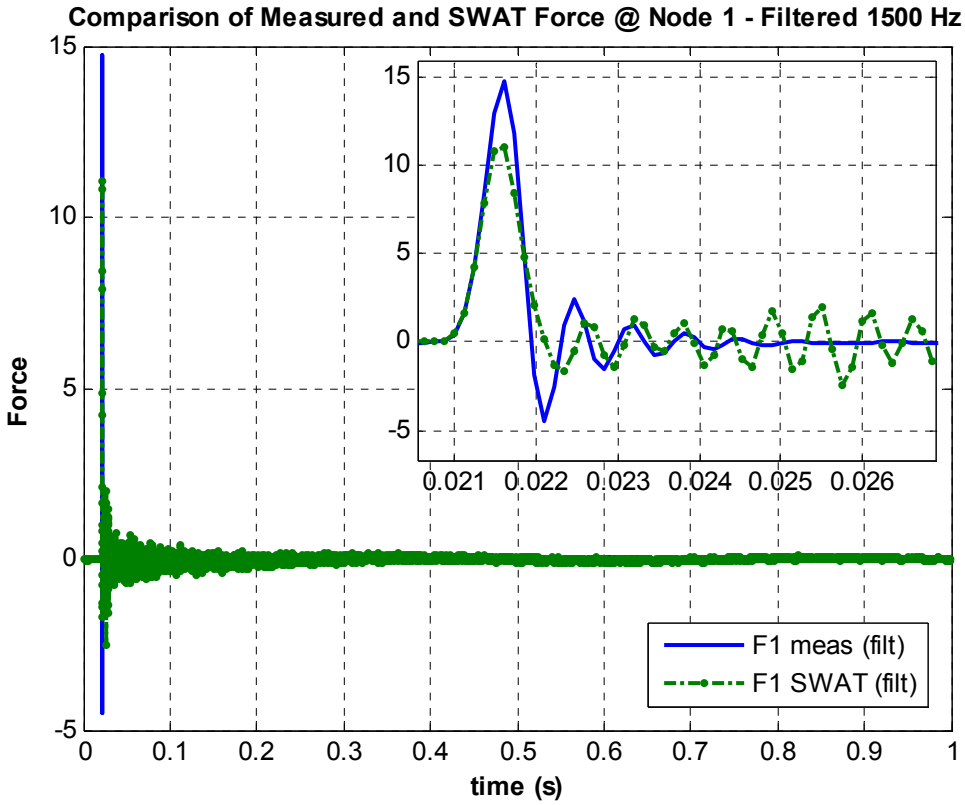

Figure 5: Force at point 1 identified by SWAT vs. Measured Force in the time domain, both filtered with a cutoff frequency of 1500 Hz. (Note that the SWAT FRFs indicate that a lower cutoff frequency should be used. A 1500 Hz cutoff frequency was used in this figure to facilitate comparison with ISF in the following section.)

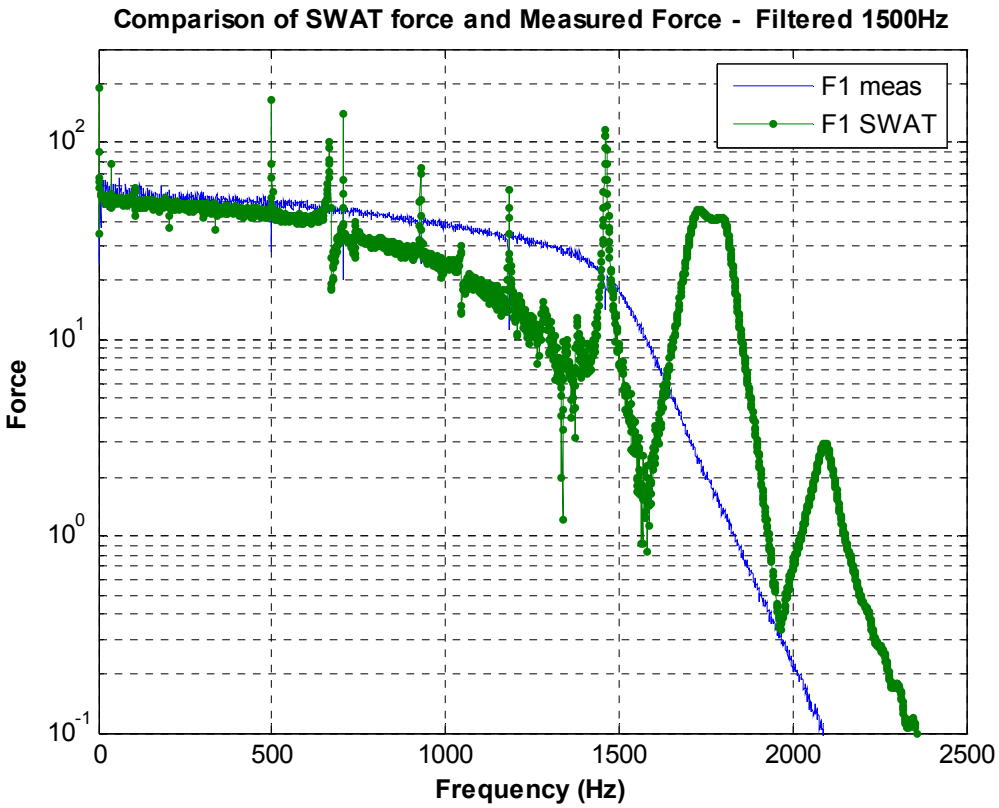

Figure 6: Force at Node 1 identified by SWAT vs. Measured Force in the frequency domain both filtered with a cutoff frequency of 1500 Hz. (Note that the SWAT FRFs indicate that a lower cutoff frequency should be used. A 1500 Hz cutoff frequency was used in this figure to facilitate comparison with ISF in the following section.)

The agreement between the measured and identified forces in Figures 5 and 6 is only fair. Figure 6 shows that there is excellent agreement out to about 600 Hz, beyond which the agreement deteriorates. As one would expect, the agreement in the time domain is excellent if both the measured force and the SWAT force are low pass filtered with a cutoff frequency of 600 Hz. This is illustrated in Figure 7.

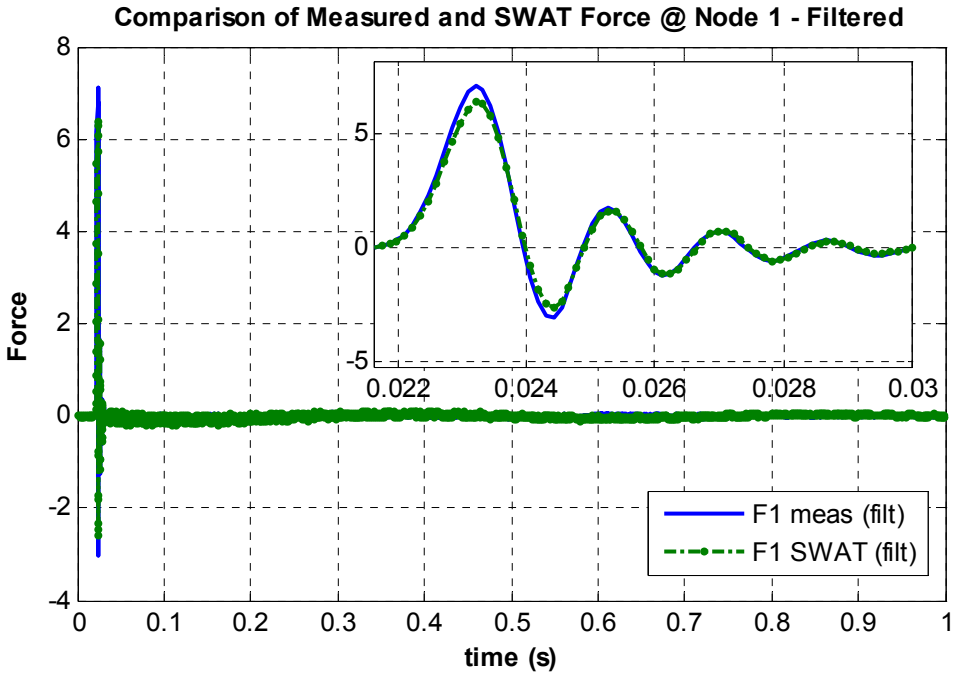

Figure 7: Force at Node 1 identified by SWAT vs. Measured Force in the time domain. The response data was filtered with a cutoff frequency of 600 Hz before applying SWAT. The measured force was also filtered for comparison.

1. Discussion

It was previously observed that the SWAT FRFs are flat out to about 600 Hz and that the 5th and 6th elastic modes occur near 500 and 700 Hz respectively. Most of the motion for this structure was in the vertical direction. With seven accelerometers in this direction and two rigid body modes, one would expect to be able to eliminate only five elastic modes. The off diagonal terms involving the sixth and higher modes suggest that the seven axial accelerometers do not provide sufficient additional information to distinguish the sixth and higher modes from the first five. These observations suggest that the SWAT algorithm can have difficulty eliminating modes that are not linearly independent in the measurement space.

It is also interesting to note that the SWAT FRFs in Figure 4 are slowly decreasing even away from the natural frequencies. This correlates with the difference between the measured and identified FRFs in Figures 2 and 11, suggesting that it could be due to the residual flexibility of modes above 1500 Hz. An attempt was made to remedy this by extracting the residual flexibility from the measured FRFs and including it as an additional mode shape in the calculation of the SWAT weights. (The residual flexibility has the form $UR*\omega^2$ where UR is a constant, see [29] or [30].)

The SWAT FRFs computed including the residual flexibility are shown in Figure 8. Comparison with Figure 4 shows that the decreasing trend is somewhat less severe, yet still present. It was observed that the residual flexibility did not entirely account for the increasing/decreasing trends observed in the residual FRFs (the difference between the measured and fit FRFs) at high frequency, suggesting that the out of band modes could not be described entirely with a residual flexibility term. Nevertheless, this does seem to confirm the hypothesis that out of band modes are at least partially responsible for the trends seen in Figures 4 and 8. These discussions also highlight the great utility of the SWAT FRFs both in providing an *a priori* indication of the expected accuracy of the identified forces and as a diagnostic tool.

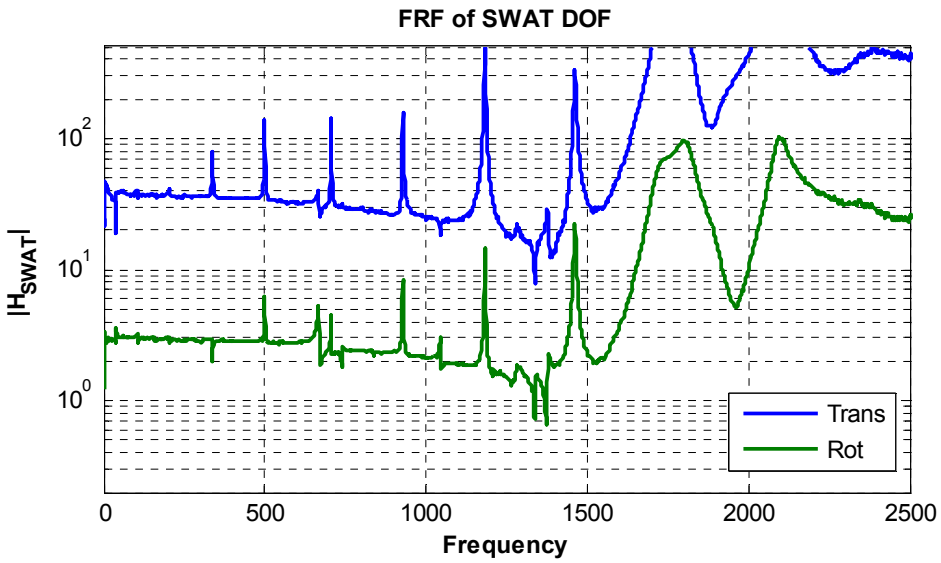

Figure 8: FRF for SWAT degrees of freedom, rigid body translation and rigid body rotation (or pitch.) including upper residual terms when deriving the SWAT weights.

B. Inverse Structural Filter

1. Impulse Response based ISF

As discussed previously, the authors are not aware of a case in which Steltzner and Kammer [10] used the equations in Section II to derive an ISF system from a forward system model. Instead, they derived a convolution representation for the ISF system directly from the measured impulse response (i.e. from the Markov parameters). This approach was attempted for this problem using the inverse FFT of the measured frequency response functions as primary data. Steltzner and Kammer suggested trying various non-causal leads to improve the performance of the ISF system. Experimentation revealed that the best results were obtained using a non-causal lead of 5 samples with 50 terms in the convolution equation. Figure 9 compares the force identified by this ISF to the measured force. During the first 22 milliseconds the ISF force tracks the measured force very well. At later times the reconstructed response becomes highly oscillatory. Various filter lengths and non-causal leads were investigated, although none resulted in better agreement between the measured and reconstructed forces than that shown in Figure 9.

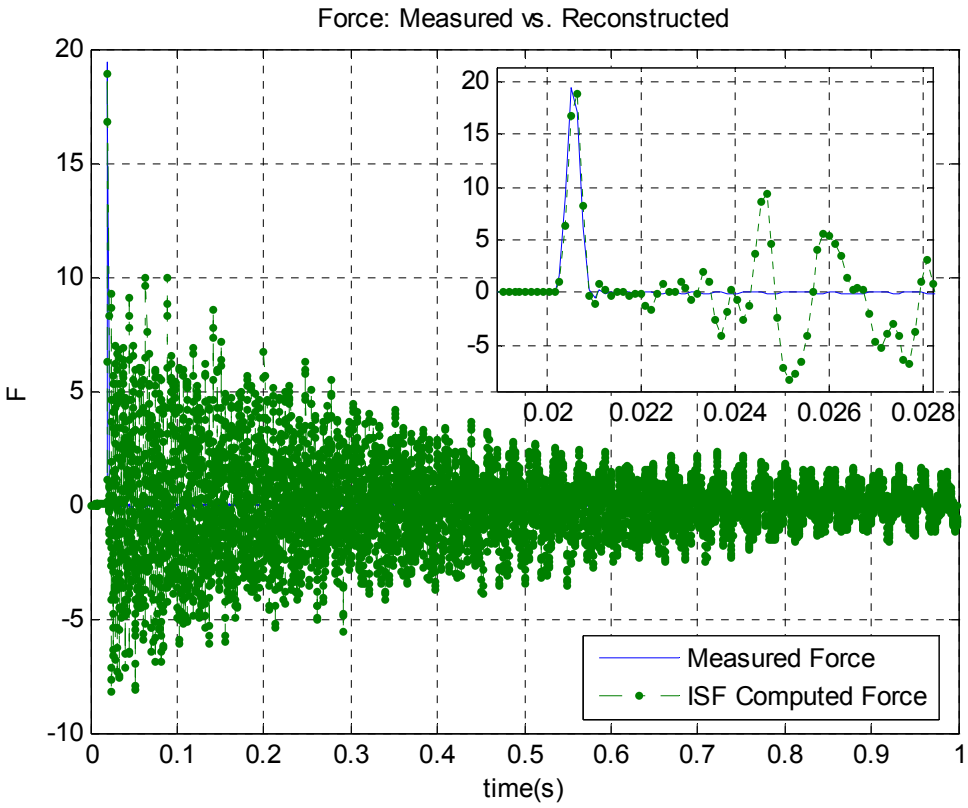

Figure 9: Input force at Node 1 estimated by ISF compared to measured force.

2. ISF Derived from Experimental Modal Model

An inverse structural filter can also be derived directly from a state space dynamic model as discussed in Section II. A state space model can accommodate a system description containing complex mode vectors (i.e. a non-proportionally damped system). To make use of this, the FRF data was curve fit using the state space version of AMI [27] to obtain a system model from which an ISF was computed. Figure 10 compares the measured drive point FRF with that reconstructed from the parameters identified by AMI. Figure 11 displays composites of the measured FRFs, AMI's reconstruction, and of the difference between the two. Comparison of Figure 11 and Figure 2 reveals that the reconstruction based on complex modes agrees much more closely with the measured data than the reconstruction based on real modes. On the other hand, comparison of Figure 8 and Figure 1 shows that the zeros of the FRF at higher frequencies do not agree as well as they did when using real modes.

A low-frequency residual term was used when curve fitting the FRFs to a complex modal model in order to describe the rigid body dynamics of the system and improve the fit near the zeros of the FRFs. A residual term was not used when curve fitting the FRFs with real modes, although inclusion of a residual term was later found to improve the agreement further for real modes also. The primary motivation for including this low-frequency residual term when fitting complex modes to the FRFs was to assure that the dynamic model used to generate the ISF system contained a representation of the dynamics of the rigid body modes. This was accomplished by assigning the real part of the low frequency residual term a very low frequency eigenvalue and including it in the state space representation in eq. (11). When this term was omitted, the forces identified by the ISF contained spurious low-frequency components of very high amplitude. These components could have been eliminated by high-pass filtering the data, yet it seems more elegant to simply include the rigid body dynamics in the system model.

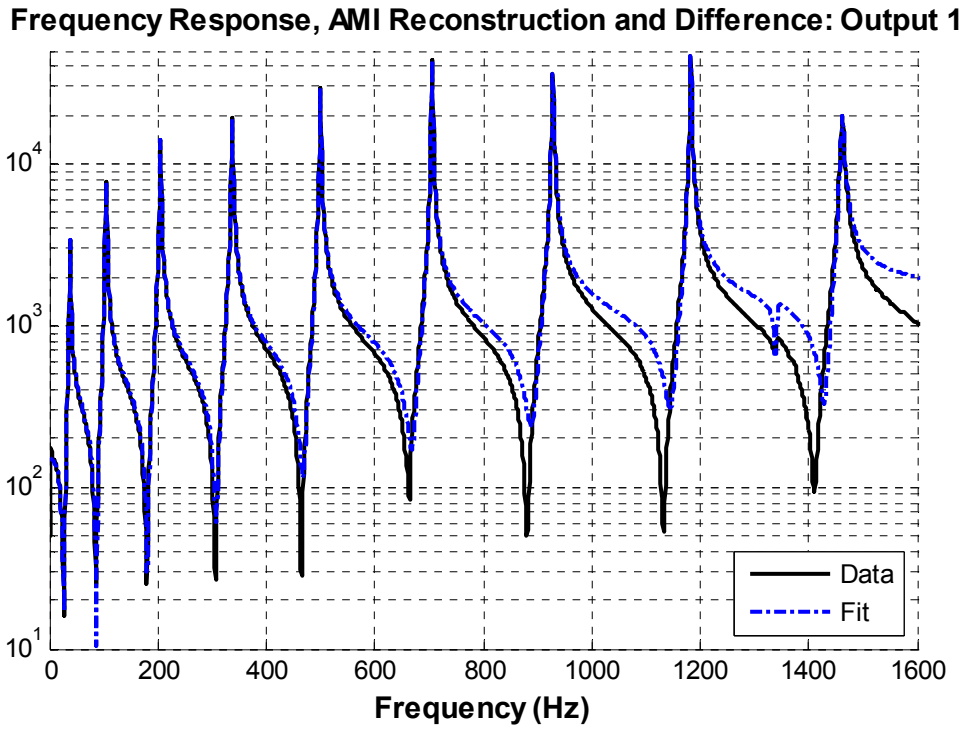

Figure 10: Measured Drive Point FRF $H_{1,1}(\omega)$ vs. AMI Reconstruction – Complex Modes with Low-Frequency Residual.

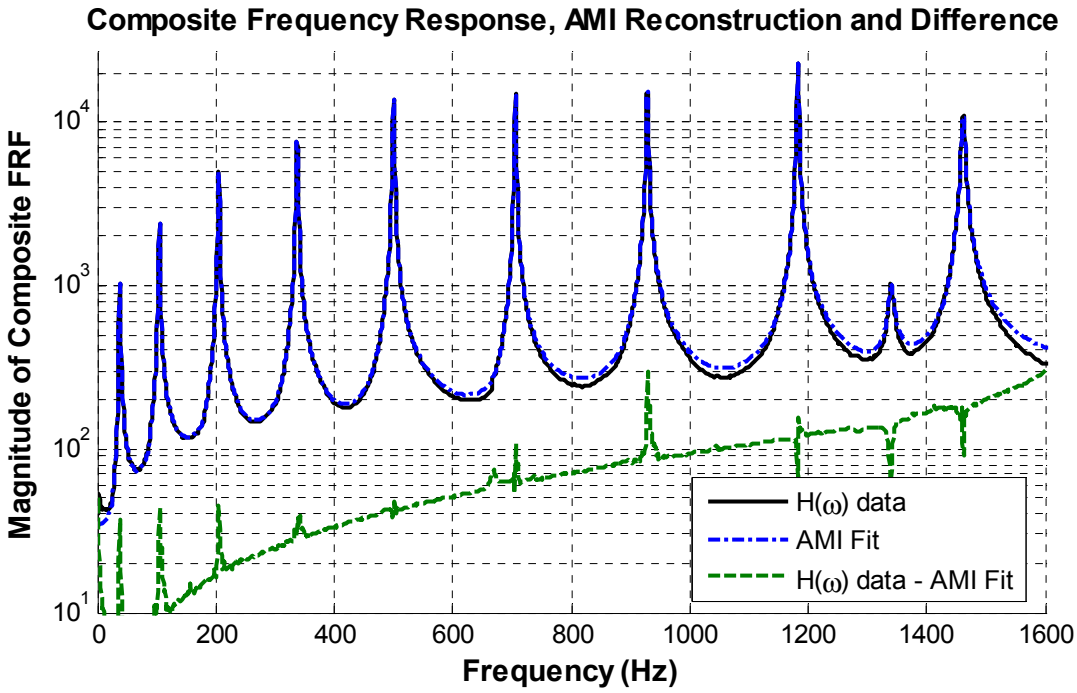

Figure 11: Composites of Measured FRFs, AMI's Reconstruction and the difference between the two – Complex Modes with Low-Frequency Residual.

The delayed, multi-step ISF method (DMISF) described in Section II.B.3 was also applied to the measured data with p=5. The ISF system was then applied to the measured response data for the beam. This result was found to be

somewhat better than that of the method presented in Section II.B.2, the result of which is shown in the appendix. Figure 12 compares the force returned by the delayed ISF with the measured force. The inverse FFT of the force obtained by the frequency domain inverse method (FD) is also shown. The agreement is excellent, although both the DMISF and FD forces show some residual ringing after the force had ceased. The ringing is slightly more severe for the DMISF method.

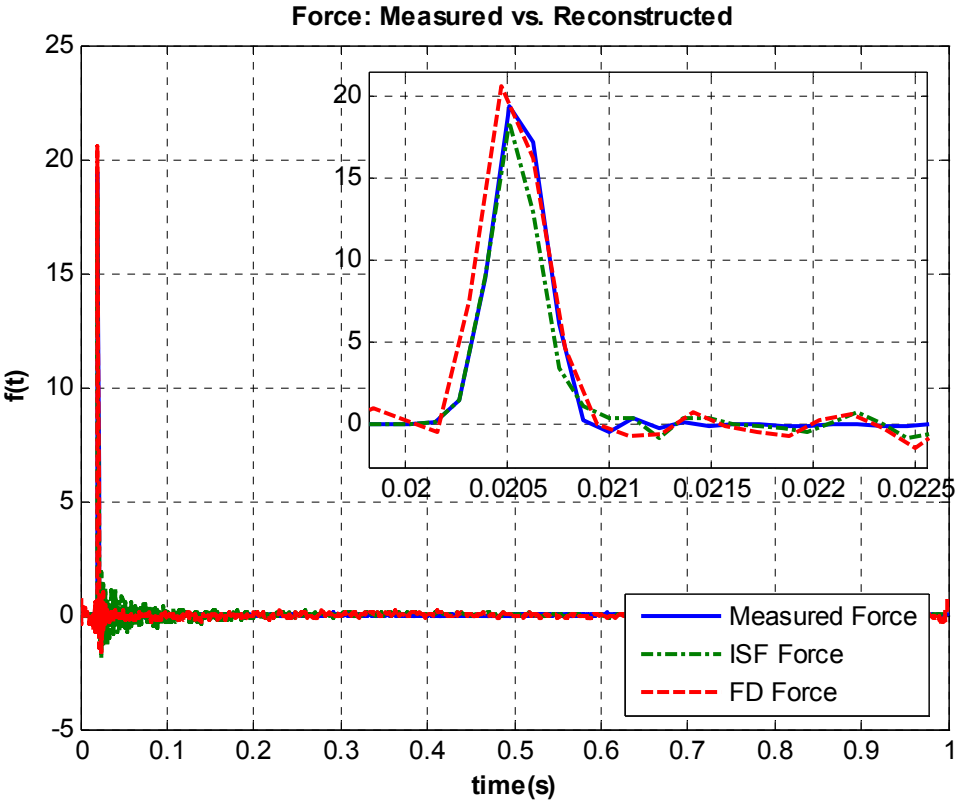

Figure 12: ISF Force, FD Inverse Method Force, and Measured Force in the time domain.

Figure 13 compares the spectra of the force identified by the DMISF to those of the measured force and the force identified by the Frequency Domain inverse method (FD). Markers are also displayed indicating the natural frequencies of the forward system (crosses) and the ISF system (circles). Both the ISF and FD forces show spikes at many of the natural frequencies of the forward system. The ISF force shows large, narrow band deviations from the measured force at many of its poles. Visual inspection suggests that the area under each of the curves is similar, indicating that each of the identified forces should impart a similar amount of energy into the structure. It is also interesting that the identified force spectrum follows the trend of the measured force even beyond the 1500 Hz curve fit band, even though the modes beyond 1500 Hz were not identified nor used in calculating the applied force.

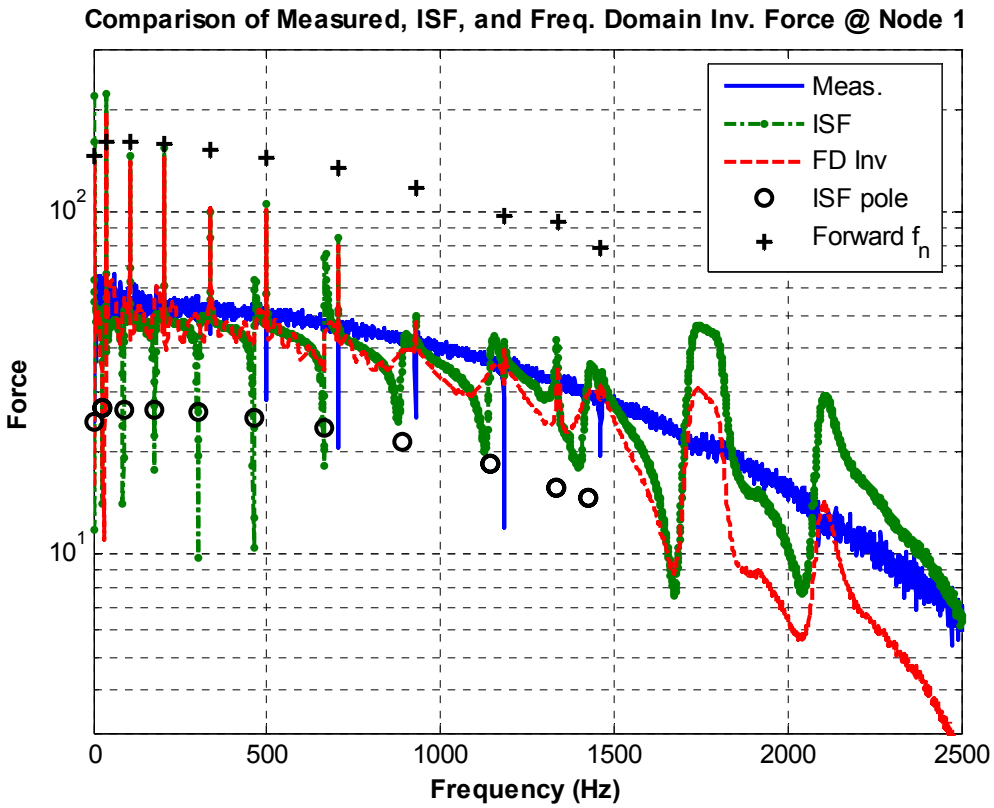

Figure 13: Measured force, FD Inv. Force and ISF Force using the DMISF method in Section II.B.3. Circles indicate the natural frequencies of the ISF system, while crosses indicate the natural frequencies of the forward system.

3. Discussion

The results presented in this section show that one can obtain similar estimates of the forces acting on a structure using either the time domain Inverse Structural Filter (ISF) method or classical Frequency Domain (FD) inverse method. The most significant difference between the two approaches stems from the poles of the ISF system, which are related to the zeros of the forward system. In some cases the ISF system generated from a set of modal parameters may have some unstable poles and be completely useless. Furthermore, Figure 13 shows that even if a stable ISF system is found, the ISF computed forces may be inaccurate at the poles of the ISF system. Fortunately, one is not resigned to failure in these cases. For example, the techniques described in Section II.B may result in a more stable and more accurate ISF system. A number of other alternatives exist; the possibilities have only been highlighted in this paper.

C. Comparison and Discussion of All Methods

Figure 14 compares the force spectra identified by all of the methods discussed in this paper. The spectrum identified by SWAT is the smoothest and most accurate below 500 Hz yet it deviates from the measured spectrum a fair amount above 500 Hz, underestimating the force by a factor of two at 1400 Hz. The other methods track the force spectrum a little more closely above 500 Hz, yet they show a number of spurious peaks. If the force spectrum was known *a priori* to be smooth (or of short duration in the time domain) then one could apply windowing or filtering to smooth the estimated spectra.

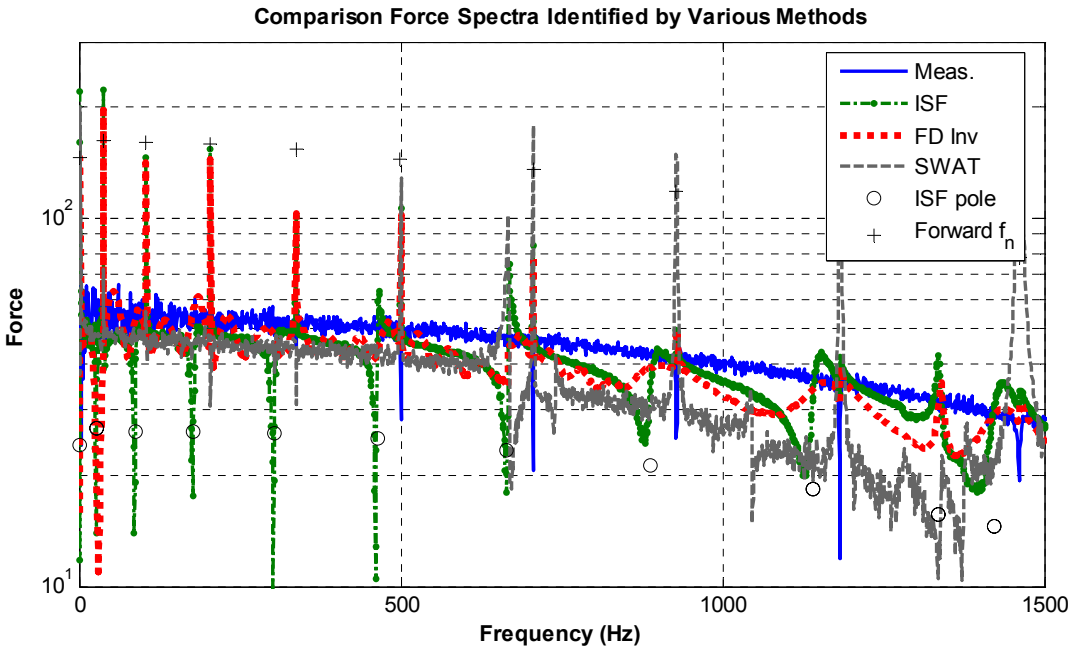

Figure 14: Comparison of forces identified by all methods.

This study has been limited to a case in which the location of the applied force was known. It is immensely important that we mention that both the ISF and frequency domain inverse methods were highly sensitive to the location at which the force was assumed to have been applied. For example, attempts were made to process the same data using the ISF method to extract the forces applied in the vertical direction at the first two measurement locations simultaneously. One would expect to recover the same estimate for the first force as found above and that the second force would be zero or near zero. On the contrary, this produced an unstable ISF and one had to go to great lengths find a stable alternative. Furthermore, even once a stable ISF was found the results were disappointing. These observations suggest that SWAT might often be the algorithm of choice in cases where the loads are moving or distributed or their locations are not precisely known.

D. Sensitivity to Errors in Identified Model

The sensitivity of all of the methods was studied using Monte Carlo simulation. The modal natural frequencies, damping ratios and residues identified were each perturbed by a uniform random number to span ±0.5%, ±5% and ±5% respectively of their identified values. These values are meant to be typical of error bounds encountered in modal parameter identification. The force spectra were then re-identified using SWAT, the delayed ISF and the frequency domain inverse method using the perturbed modal parameters to calculate the forces acting on the beam. This was repeated for 10 different sets of random perturbations. The range spanned by the identified forces as a function of time and frequency were then stored.

Figure 15 shows the range of forces identified as a function of time using all three methods. Each color band represents the maximum and minimum force observed at each particular time for the ensemble of ten responses, each force-time history corresponding to a different set of modal parameters. The particular ISF was the delayed version of Section II.B.3, which was found to be less sensitive to uncertainty than the standard formulation in Section II.B.2. The SWAT weights used in this study included the real part of the upper residual or residual stiffness, which describes the contribution of out of band modes. The responses used as input data in this study were filtered with a cutoff frequency of 1500 Hz in order to limit the contribution of the response above the frequency band that was used in system identification. The time responses all appear to be relatively insensitive to the uncertainties in the identified modal parameters. The SWAT algorithm appears to be the most sensitive to the parameter variation, although the cutoff frequency of 1500 Hz is somewhat beyond the maximum usable range of the SWAT algorithm, as discussed previously.

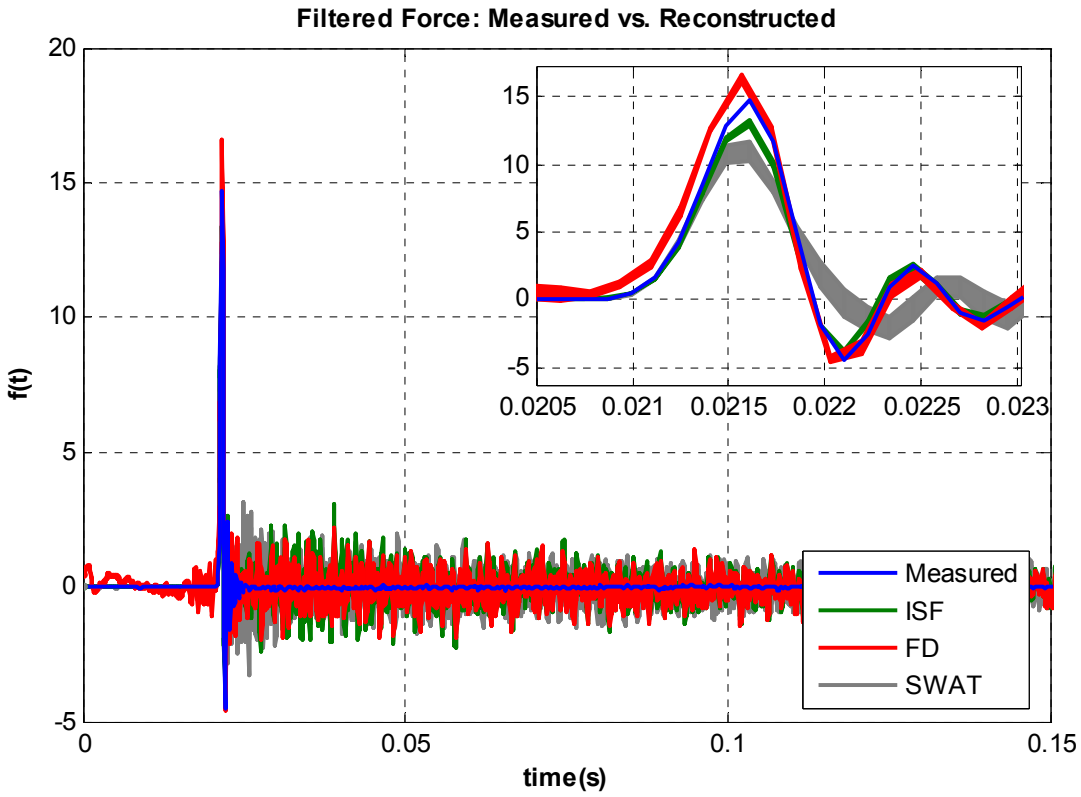

Figure 15: Range of forces found versus time for DMISF (sec. 2.2.3), Frequency Domain Inverse method and SWAT.

Figure 16 shows range of the force amplitude spectra of the forces used to create Figure 15 where, once again, each solid band represents the maximum and minimum of the ensemble of observed spectra. The SWAT algorithm shows a little more variability at the natural frequencies of the structure and a wider band of uncertainty away from the structure's natural frequencies. The Frequency domain inverse method and the ISF show similar levels of uncertainty, with the largest uncertainties at the structure's natural frequencies. The ISF algorithm also exhibits relatively large uncertainty at its poles (denoted by circles in Figure 16.) It was observed that the uncertainty at the poles of the ISF system was noticeably smaller for this ISF, which was constructed using the delayed multi-step ISF (DMISF) of Section II.B.3, than was that of the ISF in Section II.B.2. The frequency domain inverse method identified force overlays that of the ISF at many frequencies, yet at almost all frequencies where the ISF force is hidden it was found to be of equal or very similar amplitude.

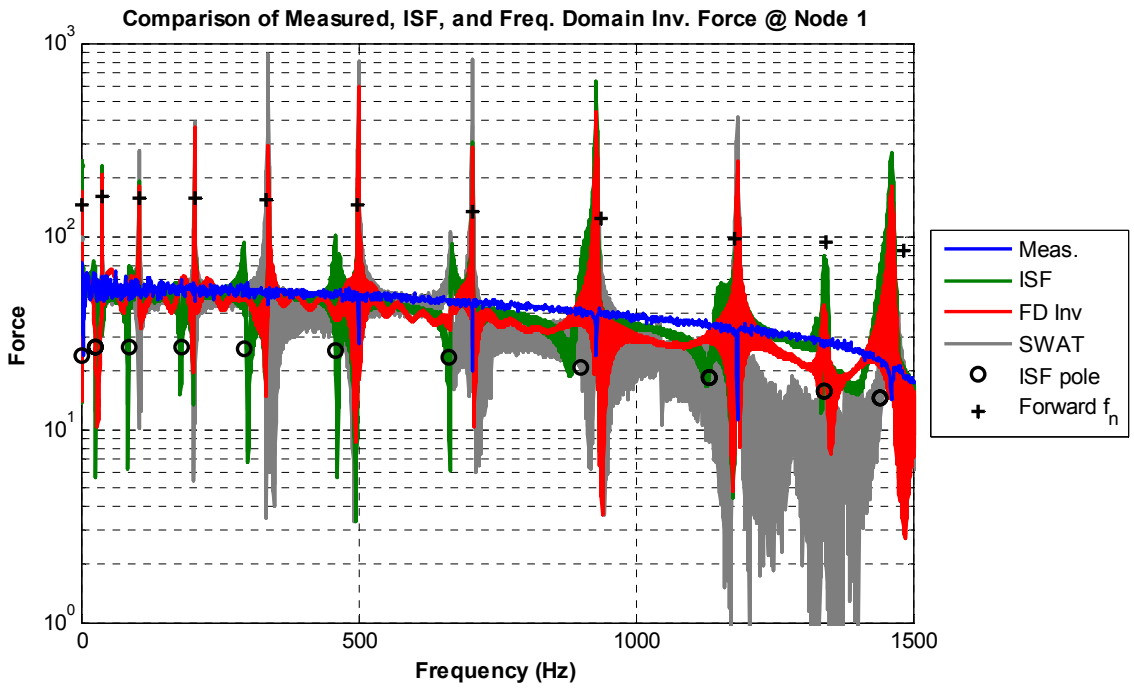

Figure 16: Range of forces found versus frequency for DMISF (sec. 2.2.3), Frequency Domain Inverse method and SWAT.

IV. Conclusions

Under the right conditions, both the SWAT and ISF algorithms can be used to estimate the forces acting on a structure in real time. Each algorithm has distinct advantages and disadvantages.

SWAT requires a sufficient number of sensors to adequately characterize the spatial nature of all contributing modes. In this application, the MAC matrix showed that the first five modes of the system (spanning 0 to 600 Hz) were quite linearly independent. It was also observed that the force identified by SWAT matched the measured force up to about 600 Hz. However, the nature of the disagreement above 600 Hz suggested that the discrepancy could be due to residual effects from out of band modes rather than inadequate spatial filtering. The most notable advantage of SWAT over the ISF and frequency domain inverse method was that SWAT did not require a highly precise and complete modal model. Only the mode shapes of the system were needed; the residual terms, which were more difficult to measure, were not as important for SWAT as they were for the ISF. In this regard, SWAT was much more robust than the other methods. One could obtain reasonable results with SWAT on the first attempt so long as the data was low pass filtered to limit the effect of modes outside of the system identification band. The other methods required multiple iterations on the curve fit model before good results were obtained. Given these observations, it is somewhat surprising that the SWAT algorithm was so sensitive to errors in the identified mode shapes, as illustrated in Section III. One would suppose that this sensitivity would decrease if more sensors were used, making the mode shapes more independent and thus allowing for improved spatial filtering. The relatively good low frequency performance of SWAT in Figure 16 seems to support this hypothesis.

The ISF algorithm was much more difficult to apply than SWAT and was sensitive to errors in the zeros of the curve fit model. The force identified in the time domain was erratic or unstable at low frequencies in early attempts, when the rigid body dynamics had not been adequately accounted for (using a lower residual term.) As alarming as this discrepancy was in the time domain, it actually covered a relatively narrow band in the frequency domain, so it should not be too much of a stumbling block for an expert user. Once a good, stable ISF system was found, the identified force was quite insensitive to variations in the modal parameters that were used to create it. The impulse response based method presented by Steltzner and Kammer was found to estimate the force well at early times, although the estimate was contaminated by the dynamics of the ISF filter at late times. A few alternative methods for creating ISF filters from an identified modal model were presented and shown to perform significantly better than the impulse response based method. Additional possibilities that may be of use in other applications have also been highlighted.

The results presented here illustrate some of the limitations of this type of analysis. The force spectra found by each of the methods had large errors near the structure's natural frequencies. The spectra of a force that is of short duration will be smooth at frequencies that are much lower than the inverse of the force's duration. When this is the case the errors near the structures natural frequencies are more of a nuisance than a real problem because they can be ignored or corrected by smoothing or windowing. On the other hand, a force spectrum that has significant narrowband components will likely be much more difficult to accurately identify.

It is often emphasized that the inverse problem is highly sensitive to errors in the parametric model for a structure, and thus implied that one should abandon any hopes of obtaining reasonable results. It is more accurate to say that the inverse problem is sensitive to errors in quantities that are not important for some other applications. Many applications of experimental modal analysis, such as FEA model validation, may be able to tolerate relatively large errors in the natural frequencies and mode shapes of the system under test, leading to much less stringent system identification requirements. On the other hand, the ISF was found to be sensitive to the zeros of the forward system and there were nuisance issues associated with the residual mass effects of modes below the frequency band of interest. Control system design and admittance modeling are two more examples of applications that can also be sensitive to errors in the estimated zeros of a system. These applications are certainly more difficult, yet one should not give up hope. More than adequate results can be obtained in many cases, especially if the limitations and sensitivities of the methods are understood and accounted for.

Appendix

A. ISF System of Section II.B.2

The method described in Section II.B.2 was used to generate an ISF system from the modal parameters identified by AMI. The spectrum of the force identified by this ISF is compared to the measured and frequency domain inverse method forces in Figure 17.

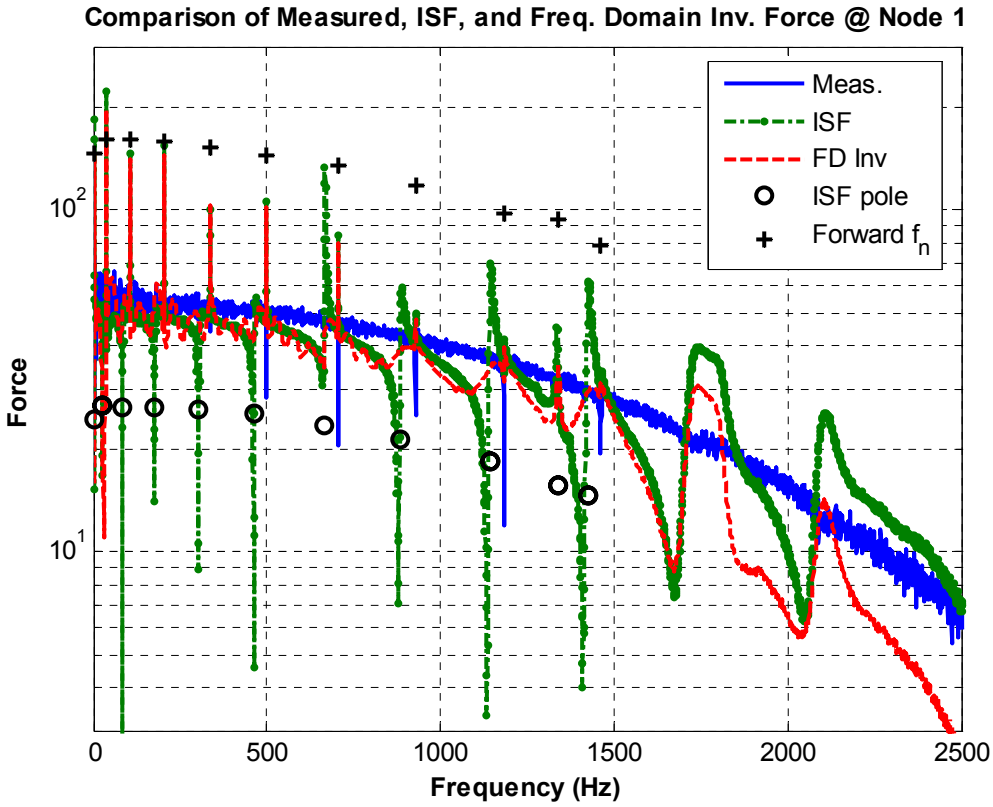

Figure 17: Measured force, ISF force and FD Inv. Force in the Frequency Domain. Circles indicate the natural frequencies of the ISF system, while crosses indicate the natural frequencies of the forward system.

Comparison of Figures 17 and 13 reveals that the DMISF force agrees a little more closely with the measured force. The authors have also found that the delayed formulation sometimes provides a stable ISF when the other methods do not and it is somewhat less sensitive to errors in the modal parameters of the identified forward system. On the other hand, this method may be adequate in some applications and requires a lower order ISF.

B. Improving Performance of ISF: Transformed Output

Another approach for generating a stable ISF stems from the observation that the zeros of the forward system (in eq. (12)), which become the poles of the ISF system, depend on the definition of the output vector. In many cases it could be possible to obtain an ISF system with stable poles by using a modified output. For example, if the transformed output

$$\{\ddot{y}_{k+1}^{new}\} = [T]\{\ddot{y}_{k+1}\} \tag{18}$$

is used in eq. (13), the ISF system matrix becomes

$$\left[\hat{A}\right] = [A] - [B]\left([T][D]\right)^{+}[T][C] \tag{19}$$

One would like to choose a transformation matrix [T] to influence the dynamics of the ISF system favorably. This is similar to the full state feedback pole-placement problem *[A]-[B][K]*, which has been treated extensively, with [K] defined as follows

$$[K] = \left([T][D]\right)^{+}[T][C] \tag{20}$$

State feedback control theory states that the eigenvalues of $\left[\hat{A}\right]$ can be placed anywhere in the complex plane through suitable choice of the state feedback gain matrix *[K]* so long as the pair *[A],[B]* is controllable. While controllability is not necessarily a problem for structural dynamic systems, one cannot necessarily find a transformation matrix *[T]* that yields an arbitrary state feedback gain matrix *[K]*. Indeed, solving for *[T]* in the equation above results in

$$\begin{aligned} &[T]\left([C] - [D][K]\right) = 0 \\ &\left([C]^T - [K]^T[D]^T\right)[T]^T = 0 \end{aligned} \tag{21}$$

which shows that one can only find a transformation matrix for a given state feedback gain matrix *[K]* if the term in parenthesis has a non-trivial null space. For example, one can place the poles of the ISF system arbitrarily if the number of measurement points N_o exceeds the order of the forward system N.

Unfortunately the authors have not found standard pole placement algorithms to be very helpful when the number of measurement points is less than the order of the system. However, they have found cases in which an unstable ISF was stabilized through judicious selection of the transformation matrix. For example, in some cases it was possible to find a transformation matrix that minimized the real part of the maximum eigenvalue of the ISF system using a Nelder-Mead optimization algorithm ("fminsearch" in Matlab.)

Acknowledgments

This work was performed at Sandia National Laboratories and supported by the US Department of Energy under contract DE-AC04-94AL85000. The authors would like to thank Eric Stasiunas for providing the test data that was used in this work.

References

[1] K. K. Stevens, "Force Identification Problems - An Overview," presented at Proceedings of the 1987 SEM Spring Conference on Experimental Mechanics, Houston, TX, 1987.

[2] R. J. Hundhausen, D. E. Adams, M. Derriso, P. Kukuchek, and R. Alloway, "Transient Loads Identification for a Standoff Metallic Thermal Protection System Panel," presented at 23rd International Modal Analysis Conference (IMAC XXIII), Orlando, Florida, 2005.

[3] J. A. Fabunmi, "Effects of Structural Modes on Vibratory Force Determination by the Pseudoinverse Technique," *AIAA Journal*, vol. 24, pp. 504-509, 1986.

[4] H. Lee and Y.-s. Park, "Error Analysis of Indirect Force Determination and a Regularisation Method to Reduce Force Determination Error," *Mechanical Systems and Signal Processing*, vol. 9, pp. 615-633, 1995.

[5] D. C. Kammer, "Input force reconstruction using a time domain technique," presented at AIAA Dynamics Specialists Conference, Salt Lake City, UT, 1996.

[6] B. Hillary and D. J. Ewins, "The Use of Strain Gauges in Force Determination and Frequency Response Function Measurements," presented at 2nd International Modal Analysis Conference (IMAC II), Orlando, Florida, 1984.

[7] E. Parloo, P. Verboven, P. Guillaume, and M. Van Overmeire, "Force Identification by means of in-operation modal models," *Journal of Sound and Vibration*, vol. 262, pp. 161-173, 2003.

[8] D. C. Kammer and A. D. Steltzner, "Structural identification of Mir using inverse system dynamics and Mir/shuttle docking data," *Journal of Vibration and Acoustics*, vol. 123, pp. 230-237, 2001.

[9] D. C. Kammer and A. D. Steltzner, "Structural identification using inverse system dynamics," *Journal of Guidance Control and Dynamics*, vol. 23, pp. 819-825, 2000.

[10] A. D. Steltzner and D. C. Kammer, "Input Force Estimation Using an Inverse Structural Filter," presented at 17th International Modal Analysis Conference (IMAC XXVII), Kissimmee, Florida, 1999.

[11] P. E. Hollandsworth and H. R. Busby, "Impact Force Identification Using the Generalize Inverse Technique," *International Journal of Impact Engineering*, vol. 8, pp. 315-322, 1989.

[12] S. S. Law and T. H. T. Chan, "Moving Force Identification: A Time Domain Method," *Journal of Sound and Vibration*, vol. 201, pp. 1-22, 1997.

[13] G. Genaro and D. A. Rade, "Input Force Identification in the Time Domain," presented at 16th International Modal Analysis Conference (IMAC XVI), Santa Barbara, California, 1998.

[14] T. G. Carne, V. I. Bateman, and R. L. Mayes, "Force Reconstruction Using a Sum of Weighted Accelerations Technique," presented at 10th International Modal Analysis Conference (IMAC X), San Diego, CA, 1992.

[15] D. L. Gregory, T. G. Priddy, and D. O. Smallwood, "Experimental Determination of the Dynamic Forces Acting on Non-Rigid Bodies," presented at Aerospace Technology Conference and Exposition, Long Beach, California, 1986.

[16] D. O. Smallwood and D. L. Gregory, "Experimental Determination of the Mass Matrix Using a Constrained Least Squares Solution," presented at AIAA/ASME SDMC Conference, Monterey CA, 1987.

[17] V. I. Bateman and T. G. Carne, "Force Reconstruction for Impact Tests of an Energy-Absorbing Nose," *The International Journal of Analytical and Experimental Modal Analysis*, vol. 7, pp. 41-50, 1992.

[18] G. H. James, "Estimation of the Space Shuttle Rollout Forcing Function," presented at 23rd International Modal Analysis Conference (IMAC XXIII), Orlando, Florida, 2005.

[19] R. L. Mayes, "Measurement of Lateral Launch Loads on Re-Entry Vehicles Using SWAT," presented at 12th International Modal Analysis Conference (IMAC XII), Honolulu, Hawaii, 1994.

[20] B. Peeters, "System Identification and Damage Detection in Civil Engineering." Leuven: Katholeike Universiteit Leuven, 2000, pp. 256.

[21] J. H. Ginsberg, *Mechanical and Structural Vibrations*, First ed. New York: John Wiley and Sons, 2001.

[22] R. L. Mayes and D. D. Johansen, "A Modal Parameter Extraction Algorithm using best-fit reciprocal vectors," presented at 16th International Modal Analysis Conference (IMAC XVI), Santa Barbara, California, 1998.

[23] R. L. Mayes and S. E. Klenke, "The SMAC Modal Parameter Extraction Package," presented at 17th International Modal Analysis Conference, Kissimmee, Florida, 1999.

[24] M. S. Allen, "Global and Multi-Input-Multi-Output (MIMO) Extensions of the Algorithm of Mode Isolation (AMI)," in *George W. Woodruff School of Mechanical Engineering*. Atlanta, Georgia: Georgia Institute of Technology, 2005, pp. 129.

[25] M. S. Allen and J. H. Ginsberg, "Global, Hybrid, MIMO Implementation of the Algorithm of Mode Isolation," presented at 23rd International Modal Analysis Conference (IMAC XXIII), Orlando, Florida, 2005.

[26] M. S. Allen and J. H. Ginsberg, "Modal Identification of the Z24 Bridge Using MIMO-AMI," presented at 23rd International Modal Analysis Conference (IMAC XXIII), Orlando, Florida, 2005.

[27] M. S. Allen and J. H. Ginsberg, "A Global, Single-Input-Multi-Output (SIMO) Implementation of The Algorithm of Mode Isolation and Applications to Analytical and Experimental Data," *Mechanical Systems and Signal Processing*, vol. 20, pp. 1090–1111, 2006.

[28] R. J. Allemang, *Vibrations Course Notes*. Cincinnati: http://www.sdrl.uc.edu/, 1999.

[29] W. Heylen, S. Lammens, and P. Sas, *Modal Analysis Theory and Testing*. Leuven, Belgium: Katholieke Universiteit Leuven, 2000.

[30] B. Peeters, P. Guillaume, H. Van Der Auweraer, B. Cauberghe, P. Verboven, and J. Leuridan, "Automotive and aerospace applications of the PolyMAX modal parameter estimation method," presented at International Modal Analysis Conference (IMAC XXII), Dearborne, Michigan, 2004.